Corrosion Protection by Octadecylphosphonic Acid in Flow Conditions

E. Kristan Mioč and H. Otmačić Ćurković*
Faculty of Chemical Engineering and Technology,
University of Zagreb, Marulićev trg 19,
10000 Zagreb, Croatia

https://doi.org/10.15255/CABEQ.2018.1572
Original scientific paper
Received: December 30, 2018
Accepted: September 16, 2019

The aim of this work was to examine the influence of the flow rate of corrosive media on the stability of self-assembled films of octadecylphosphonic acid on copper-nickel alloy and stainless steel. The studies were conducted in river and seawater in a laboratory scale flow system. Corrosion behaviour of protected and unprotected alloys was examined by electrochemical techniques, electrochemical impedance spectroscopy, and polarization measurements. The results show that octadecylphosphonic acid films can efficiently protect copper-nickel and stainless steel from corrosion in flowing natural waters. The flow of corrosive media had the highest influence on the stability of films on CuNi in seawater, while in all other studied cases, the protective properties of ODPA film changed insignificantly with the change of the flow rate.

Keywords:
corrosion protection, electrochemical measurements, river water, seawater, flow condition

Introduction

Many industrial plants, either onshore or offshore, such as plants for water conditioning and desalination, oil, paper, food, and nuclear industries and oil platforms, often use seawater or river water for various purposes, for example, as a coolant in heat exchangers. Although highly resistant alloys, such as cupronickel alloy or stainless steel, are used for designing these plants and equipment, they are still subjected to different corrosion processes. Their service life in such aggressive environments can be prolonged by protection with corrosion inhibitors. However, the marine environment is sensitive to toxic compounds that are often used as corrosion inhibitors.

Phosphonic acids are known for their spontaneous self-assembly on oxidized substrates. They easily chemisorb on many metals and alloys, and show good resistance to hydrolysis. Therefore, they represent a potentially ecologically suitable solution for increasing corrosion resistance of alloys under corrosive conditions.[1–3] Most of the studies on phosphonic acids' self-assembled monolayers (SAMs) are focused on characterization of their physical properties, SAM structure, and initial corrosion protection;[1–5] however, there is still a lack of research on their stability under realistic application conditions. Moreover, many studies have been conducted on pure metals, while studies on alloys are much scarcer. In our recent studies, it was found that it is possible to protect cupronickel alloy as well as stainless steel from the corrosive influence of artificial sea water by forming thin, self-assembled films of octadecylphosphonic acid (ODPA).[6,7]

One of the parameters influencing the corrosion of equipment materials is flow velocity, through its effect on mass transfer and other phenomena such as erosion-corrosion. The flow of corrosive medium can have two opposite effects on the efficiency of corrosion inhibitor. On the one hand, it can increase the transport of corrosion inhibitor towards the metal surface, and on the other hand, it can increase the transport of the corrosive species or dissolution of protective surface layer. Above the critical flow rate, corrosion inhibitors may lose their effectiveness, which depends on the nature and molecular structure of the inhibitor as well as on its concentration and temperature.[8–13] The aim of this work was to study the effect of the electrolyte flow rate on corrosion of unprotected and phosphonic-acid-modified cupronickel and stainless steel alloys in natural seawater and river water.

Materials and methods

Sample preparation

Investigations were performed on a cupronickel alloy rod, Cu70Ni30 (CuNi) and on a stainless steel rod, AISI 316L (SS). In order to prepare working electrodes, rods were cut out in 0.5 cm thick

*Corresponding author: E-mail: helena.otmacic@fkit.hr

samples, and on their reverse side, a copper wire was soldered. They were then embedded into epoxy resin, and the exposed surface of SS and CuNi working electrode were 1.13 and 1.33 cm^2, respectively. The electrodes were abraded with emery paper grade 800, 1200, and 2500, and polished with α-Al_2O_3 particle size 0.1 μm, degreased with ethanol in ultrasonic bath, and rinsed with deionised water. The SAM formation was carried out by the following procedure: oxide formation, 24 h at 80 °C for cupronickel and 24 h at room temperature for stainless steel, followed by spraying the samples 5 times with ODPA solution, and the drying step, 5 h at 80 °C. Acid adsorption occurred in 0.01 mol dm^{-3} octadecylphosphonic acid ethanolic solution. Studies of phosphonic acid SAMs on stainless steel and cupronickel alloy have mainly been performed with the dip-coating method, which is time-consuming, requires higher amounts of working solution, and is not always practical for application in industry. Spraying is more practical than the above-mentioned method, and in the previous studies[6], it has shown similar or even better results in corrosion protection of studied alloys. For comparison, blank samples were prepared, on which a native oxide layer was formed during 24 h at 80 °C (CuNi) or room temperature (SS). The oxidation and drying were conducted in an air convection oven.

Electrochemical measurements

Electrochemical investigations were conducted in a three-electrode cylindrical electrochemical cell, in natural seawater, sampled near the city of Zadar, and in Sava river water sampled near the city of Zagreb. The pH value of seawater was 8.2, and the pH of the river water was 7.8. Saturated calomel electrode was used as a reference electrode and graphite electrode was used as a counter electrode. All potentials in the text are referenced against saturated calomel electrode (SCE). Prior to electrochemical measurements, the electrodes were immersed in the test solution for one hour to stabilize the open circuit potential. The cell was connected to a pump and a flowmeter to fix the flow at controlled values. Experimental equipment is presented in Fig. 1.

Measurements were performed without flow, and at three different flow rates: 0.8 L min^{-1}, 1.6 L min^{-1}, and 2.4 L min^{-1}. Diameter of the cell was 4.5 cm, and surface of the full section was 0.00159 m^2. According to this surface and the three flow rates previously mentioned, the investigated velocities of the solution in the cell were 0.0084 m s^{-1}, 0.0168 m s^{-1}, and 0.0252 m s^{-1}. The polarization measurements were performed in the narrow (± 20 mV vs. E_{oc}) potential range, with a potential scan rate of 0.166 mV s^{-1}. The electrochemical impedance spectroscopy (EIS) was performed at open circuit potential (E_{oc}) in the frequency range 100 kHz – 10 mHz with a 10 mV_{rms} amplitude. The obtained impedance spectra were interpreted on the basis of equivalent electrical circuits using ZSimpWin software. In general, $\chi 2$ value was always below $5 \cdot 10^{-4}$. The electrochemical measurements were performed using a BioLogic SP-300 potentiostat. All the measurements were conducted in triplicate.

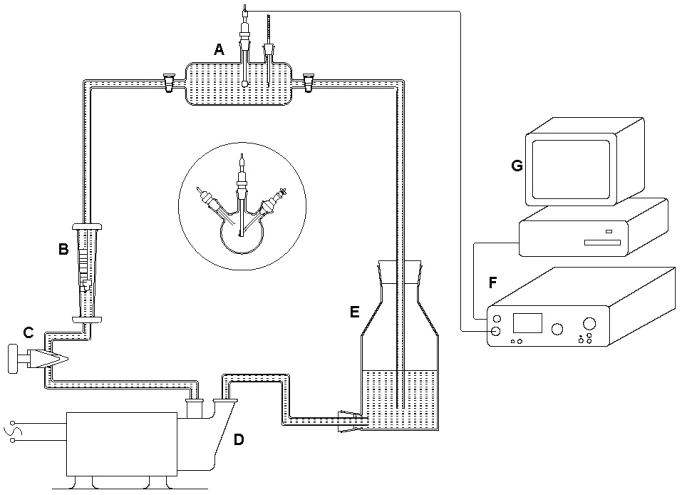

Fig. 1 – *Equipment for electrochemical measurement under flow regime: (A) flow-through cell with three electrodes, (B) flowmeter, (C) valve, (D) pump, (E) vessel, (F) potentiostat, and (G) computer*[13]

Results and discussion

Influence of media flow rate on the stability of unprotected and ODPA-modified alloys

Cupronickel alloy

In order to evaluate the influence of natural media flow rate on stability of the prepared layers of octadecylphosphonic acid, untreated and treated samples were exposed to river and seawater without flow (0 L min^{-1}), as well as at a flow rate of 0.8, 1.6, and 2.4 L min^{-1}. Polarization resistance dependence on media flow rate determined from the polarization measurements for untreated and ODPA-modified cupronickel alloy is presented in Fig. 2.

From Fig. 2, it is evident that, in both media, the protective films efficiently protected copper-nickel substrate at all studied flow rates. For the untreated samples, polarization resistance values decreased with increasing flow rates in both studied media. The decrease in polarization resistance implies an increase in the corrosion rate, which could be related to the increase in the rate of cathodic corrosion reaction, anodic corrosion reaction or both corrosion reactions. In river water, the anodic reaction is expected to result in Cu_2O formation:

$$2Cu + H_2O \rightleftarrows Cu_2O + 2H^+ + 2e^- \quad (1)$$

while cathodic reaction for this system was oxygen reduction, which probably remained under complete charge transfer control at potentials close to the corrosion potential.

$$O_2 + 2H_2O + 4e^- \rightleftarrows 4OH^- \quad (2)$$

Examination of open circuit potential variation with the flow rate change showed that, with an increase in flow rate, the open circuit potential shifted towards more negative values (from –0.055 V vs. SCE at stagnant conditions to –0.096 V vs. SCE at the highest flow rate). This change indicates that anodic reaction rate increased more significantly with the flow rate increase. While reaction (1) was not expected to be influenced by the electrolyte flow, studies[14] have shown that further oxidation of Cu_2O can lead to formation of soluble Cu(II) species whose removal from the surface can be enhanced by the electrolyte flow. On the other hand, some studies have shown that, in alkaline solutions, the formation of soluble $Cu(OH)_n^{1-n}$ species is also possible.[15] Thus, it can be assumed that increase in electrolyte flow results in faster removal of soluble corrosion products from the metal surface enabling its faster dissolution.

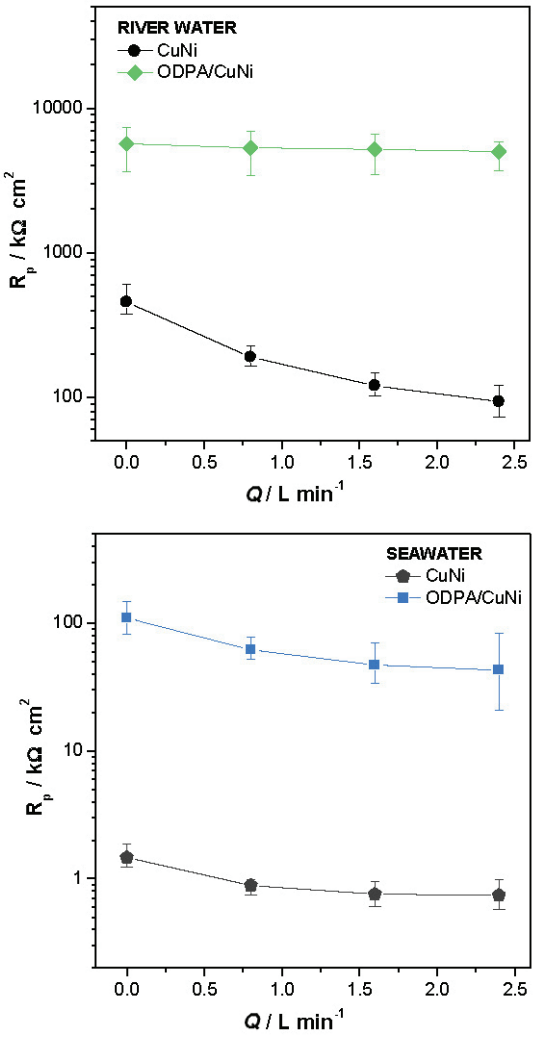

Fig. 2 – *Polarization resistance dependence on river and seawater flow rate for untreated and ODPA-modified cupronickel alloy*

The mechanism of Cu electrodissolution in chloride media has been investigated by many researchers.[16–20] At chloride concentrations lower than 1 M, the mechanism of copper dissolution can be expressed as:

$$Cu + Cl^- \rightleftarrows CuCl + e^- \quad (3)$$

$$CuCl + Cl^- \rightleftarrows CuCl_2^- \quad (4)$$

Flow of the electrolyte enhances the $CuCl_2^-$ transport from the metal surface, and thus enables faster dissolution of CuCl layer. Kear *et al.*[21] concluded that the presence of surface film can reduce both anodic and cathodic charge transfer processes. This is in agreement with the fact that, in our work, no significant change in open circuit potential with the change in the flow rate was observed, despite the change in R_p values.

For samples protected by ODPA film, the flow rate of river water had almost negligible influence on CuNi polarization resistance. This confirmed that the protective film of phosphonic acid was not destroyed by the electrolyte flow, and that it represented an efficient barrier towards diffusion of corrosive species as well as the dissolution of oxide layer. The polarization resistance values for treated samples in the seawater decreased with an increase in flow rate, but they remained significantly higher than those for blank samples. This confirmed that self-assembled films were resistant to the flow of natural media at the investigated flow rates.

Electrochemical impedance spectroscopy measurements were conducted in order to better understand corrosion behaviour of studied samples. Impedance spectra obtained for blank and ODPA-treated samples in river water are presented in Fig. 3.

The impedance curves given in Fig. 3, show the trend in the decrease of impedance value of the untreated CuNi sample by increasing river water flow rate, while for treated samples, the impedance values are similar and do not depend on the flow of water. Fitting of the impedance data for all samples required the use of an electrical equivalent circuit with two time constants. Due to the frequency dispersion, the capacitor element in electrical equivalent circuit was replaced with the constant phase element (CPE). The impedance of CPE is defined as $Z_{CPE} = 1/[Q(j\omega)^n]$, where constant Q is the frequency-independent parameter of the CPE, which

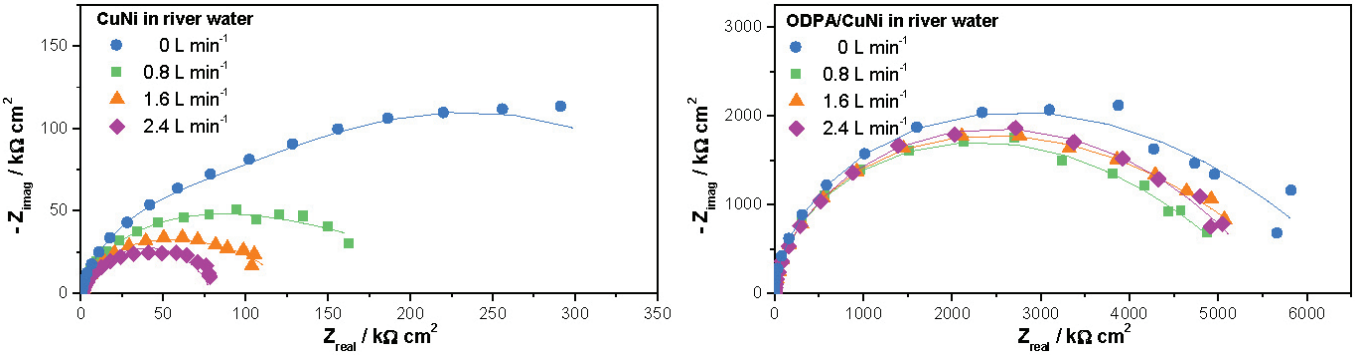

Fig. 3 – *Nyquist plots of EIS spectra for blank and ODPA-treated CuNi alloy at different river water flow rates. Dots represent experimental data, and lines represent the fitted data obtained by fitting the spectra to models given in Fig. 4.*

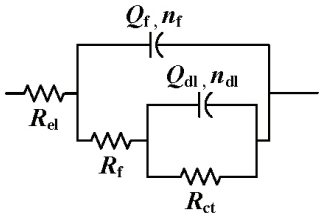

Fig. 4 – *Equivalent electrical circuits used for fitting the EIS spectra in Fig. 3*

represents pure capacitance when $n = 1$.[22] Proposed $2RQ$ circuit (Fig. 4) used for fitting EIS spectra consisted of $R_f - Q_f$ and $R_{ct} - Q_{dl}$ couples. $R_f - Q_f$ couple describes a time constant observed at high frequencies, where R_f corresponds to the resistance of the oxide film, and Q_f is related to the capacitance of the film associated with the dielectric property of this film. For treated samples, a similar model was used; however, in this case, R_f represented resistance of the pores in ODPA film, and C_f the capacitance of the surface film. $R_{ct} - Q_{dl}$ couple represents the corrosion reaction at the metal substrate/solution interface, where R_{ct} is charge transfer resistance and Q_{dl} is the constant phase element representing the double layer capacitance. The electrolyte resistance between the working and reference electrodes is represented by R_{el}.

EIS parameters obtained by fitting EIS spectra to selected equivalent circuit are given in Table 1. Since Q value is inversely proportional to the thickness of the film, for the blank CuNi sample it may be seen that the increase in the flow rate decreased the thickness of the oxide film with a decrease in the film resistance and charge transfer resistance. This is clear confirmation of the improved mass transfer of corrosive species, as well as the deterioration of protective oxide film. For treated sample, impedance parameters showed that flow had only slight effect on inhibitor film resistance, and not much on the charge transfer resistance. It may be assumed that flow induces the formation of defects in the film; however, not in a manner as to enable significant dissolution of the metallic substrate. Values of n_{dl} around 0.5 indicated that mass transfer influenced the corrosion process, which is in accordance with the previous assumption that ODPA film represents an efficient barrier towards diffusion of corrosive species as well as the dissolution of oxide layer.

Impedance spectra obtained for blank and ODPA-treated sample in seawater are presented in Fig. 5. It may be seen that impedance decreased with the increase in seawater flow rate, consistent with previous results of polarization measurements.

Table 1 – *Impedance parameters obtained for CuNi alloy in river water*

		Q_f / μS s^n cm^{-2}	n_f	R_f / kΩ cm^2	Q_{dl} / μS s^n cm^{-2}	n_{dl}	R_{ct} / kΩ cm^2
CuNi	0 L min^{-1}	1.92	0.89	92.05	7.58	0.53	427.4
	0.8 L min^{-1}	2.70	0.87	78.81	14.77	0.59	120.9
	1.6 L min^{-1}	3.37	0.85	58.75	19.13	0.54	70.4
	2.4 L min^{-1}	4.24	0.83	50.22	25.76	0.70	36.1
ODPA/CuNi	0 L min^{-1}	0.06	0.97	2791	0.25	0.50	3944
	0.8 L min^{-1}	0.06	0.97	2209	0.26	0.50	3360
	1.6 L min^{-1}	0.06	0.96	2364	0.28	0.50	3679
	2.4 L min^{-1}	0.07	0.96	1814	0.17	0.51	3923

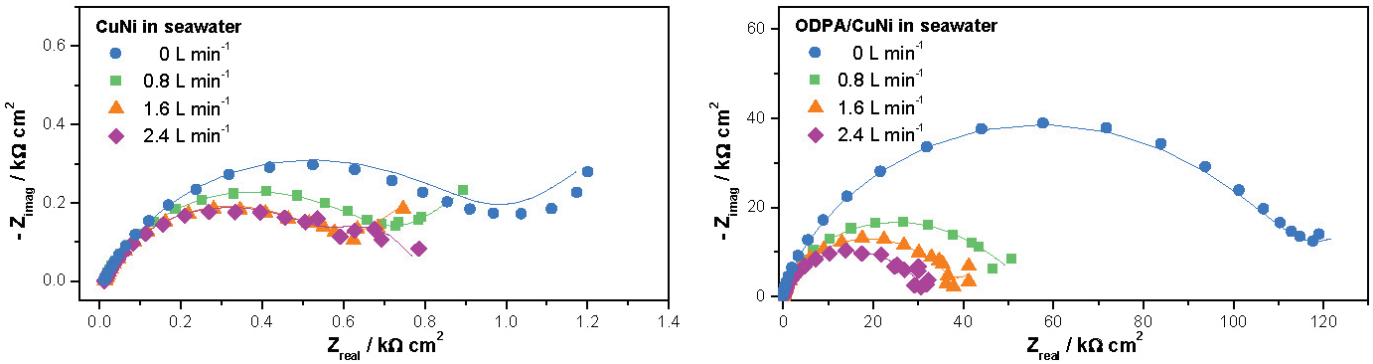

Fig. 5 – *Nyquist plots of EIS spectra for blank and ODPA-treated CuNi alloy in different seawater flow rates. Dots represent experimental data, and lines represent the fitted data obtained by fitting the spectra to models given in Fig. 6.*

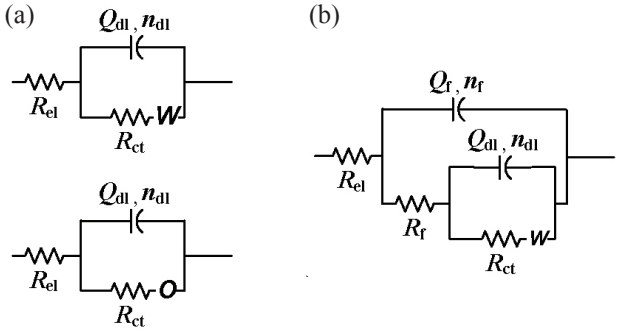

Fig. 6 – *Equivalent electrical circuits used for fitting the EIS spectra of (a) blank, and (b) ODPA-treated samples*

All spectra exhibited one phase maximum at medium frequencies and one at the lowest frequencies. The first one was ascribed to electrochemical reaction occurring at the metal – electrolyte interface, while the second was ascribed to diffusion process. Therefore, EIS spectra of blank sample were modelled with the electrical equivalent circuits presented in Fig. 6(a), where R_{ct} represents charge transfer resistance; Q_{dl} constant phase element describing the double layer capacitance, and n_{dl} corresponding coefficient. For the three lower flow rates, the low frequency region was better fitted with the Warburg impedance model (W) describing semi-infinite diffusion process, while for the highest flow rate, it was better described with finite-diffusion element (O).[23] EIS spectra of the treated sample were modelled with the 2RQW electrical equivalent circuits presented in Fig. 6(b), due to the presence of additional phase maximum at highest frequencies. The additional circle of the aforementioned model describes a film on the surface of metal, and consists of the capacitance and the resistance of the ODPA film (Q_f and R_f). The obtained impedance parameters are presented in Table 2.

It can be observed that all impedance parameters for blank CuNi sample changed with the change in the flow rate (except n_{dl}). While double layer capacitance increased with an increase in flow rate, charge transfer resistance and diffusion impedance decreased. This is clear confirmation of the improved mass transfer of corrosive species, like O_2 and Cl^-, towards the metal surface, as well as the transfer of $CuCl_2^-$ from the surface. For treated samples in general, capacitive values increased and

Table 2 – *Impedance parameters obtained for CuNi alloy in seawater*

		Q_{dl} / μS s^n cm^{-2}	n_{dl}	R_{ct} / kΩ cm^2	W / μS s$^{0.5}$ cm^{-2}		Q / μS s$^{0.5}$ cm^{-2}	O / s$^{0.5}$
CuNi	0 L min^{-1}	177.8	0.72	0.90	9017		–	–
	0.8 L min^{-1}	215.7	0.73	0.69	11620		–	–
	1.6 L min^{-1}	257.1	0.72	0.58	12870		–	–
	2.4 L min^{-1}	266.6	0.73	0.56	–		11190	2.42
		Q_f / μS s^n cm^{-2}	n_f	R_f / kΩ cm^2	Q_{dl} / μS s^n cm^{-2}	n_{dl}	R_{ct} / kΩ cm^2	W / μS s$^{0.5}$ cm^{-2}
ODPA/CuNi	0 L min^{-1}	0.74	0.88	34.36	1.84	0.60	81.39	244.8
	0.8 L min^{-1}	1.64	0.87	16.88	5.54	0.53	36.63	761.2
	1.6 L min^{-1}	2.00	0.86	17.44	5.82	0.64	20.17	555.9
	2.4 L min^{-1}	2.50	0.86	12.14	9.39	0.52	19.91	1362.0

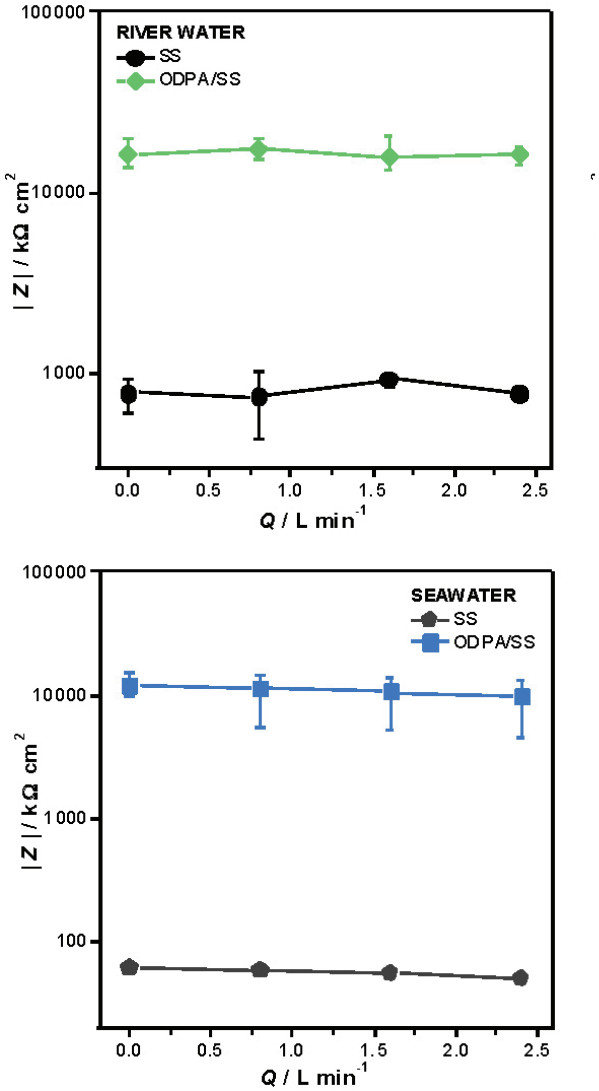

Fig. 7 – *Polarization resistance dependence on river and seawater flow rate for untreated and ODPA-modified stainless steel alloy*

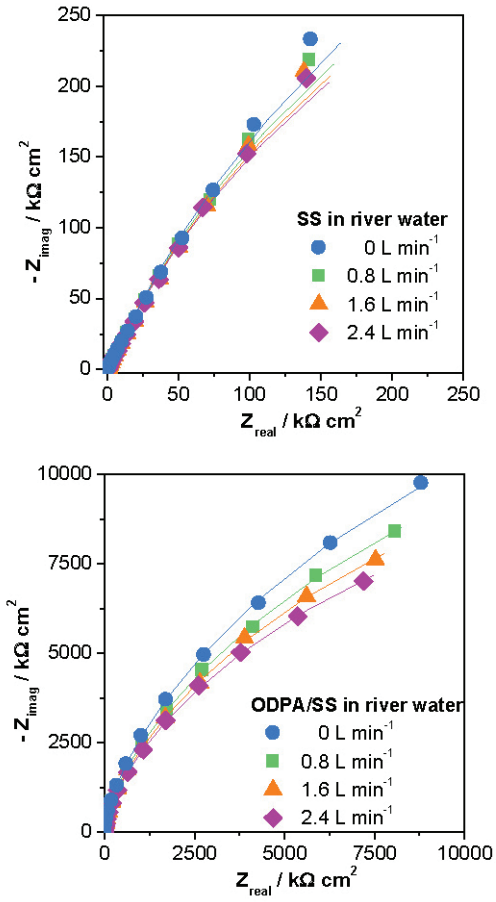

Fig. 8 – *Nyquist plots of EIS spectra for blank and ODPA-treated stainless steel in different river water flow rates. Dots represent experimental data, and lines represent the fitted data obtained by fitting the spectra to models given in Fig. 9.*

resistance values decreased with increase in flow rate. Flow of the seawater showed a more destructive effect on ODPA film than the river water. However, the obtained resistance values for treated samples were much higher than those observed for the blank sample.

Stainless steel

After examining the stability of ODPA films on CuNi alloys, the experiments were carried out on stainless steel. Polarization resistance dependence on media flow rate determined from the polarization measurements for untreated and ODPA-modified stainless steel is presented in Fig. 7.

While studies on CuNi showed significant influence of the flow rate on alloy corrosion in both studied media, for SS the influence of flow rate was much lower. This is in accordance with the studies of Mansfeld *et al.*[24], who have reported, for AISI 304 and AISI 316 under flow conditions (rotating cylinder electrode experiments), that the oxygen reduction reaction was charge-transfer-controlled and the passive current density was independent of rotation speed. Fig. 7, suggests that, in both corrosive media, there was almost no deterioration of protective films at studied flow rates, as the values of polarization resistance remained relatively stable and significantly higher compared to the values of untreated samples.

Electrochemical impedance spectroscopy measurements were conducted in order to better understand corrosion behaviour of studied samples. Impedance spectra obtained for blank and ODPA-treated samples in river water are presented in Fig. 8.

The impedance curves given in Fig. 8, show the trend of slight decrease in the impedance value of the untreated and treated stainless steel samples by increasing river water flow rate. Fitting of the impedance data for all samples required the use of an electrical equivalent circuit with two time constants given in Fig. 9, which consisted of an outer

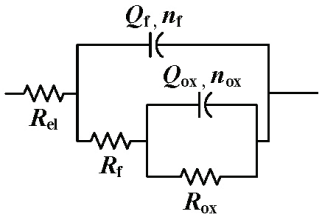

Fig. 9 – *Equivalent electrical circuits used for fitting the EIS spectra in Fig. 8 and Fig. 10*

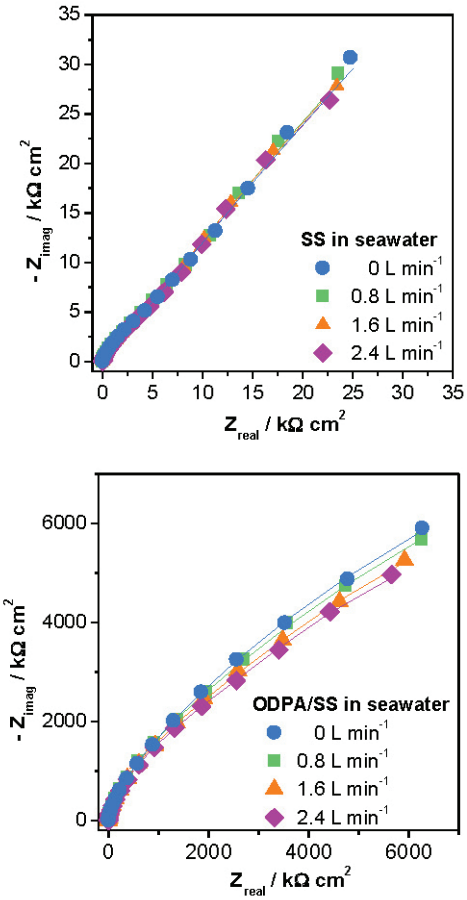

Fig. 10 – *Nyquist plots of EIS spectra for blank and ODPA-treated stainless steel in different seawater flow rates. Dots represent experimental data, and lines represent the fitted data obtained by fitting the spectra to models given in Fig. 9.*

porous and an inner compact oxide film. In case of the ODPA-treated samples, R_f–Q_f couple represents properties of ODPA film.

Impedance parameters obtained by fitting experimental data to equivalent circuits are given in Table 3. From the obtained results, a slight decrease in the thickness and resistance values of the porous and compact oxide layer on bare SS were observed with increased flow of medium. In addition, for ODPA-treated samples, a slight decrease in the film and charge transfer resistance with increased flow of media was observed. It should be emphasized that the obtained resistance values for treated samples were much higher than those observed for the blank samples, suggesting that the ODPA films effectively protected stainless steel at all tested flow rates of river water.

By analysing the impedance curves obtained for the seawater, a slight decrease or no change in the impedance value was observed with increased seawater flow rate. Fitting of the impedance data for all samples also required the use of an electrical equivalent circuit with two time constants.

The results given in Table 4 for the blank SS sample show the trend in Q_f and Q_{ox} increase, i.e., reduction in the thickness of the outer porous and inner compact oxide film, with a decrease in the resistance of both films with increased seawater flow. The results given in the table for the treated samples, suggest that, although there was a rise in the resistance of the protective film by increased seawater flow rate, no significant changes in the thickness of the film had occurred. Likewise, although there was a decrease in the resistance of the oxide film with the increase in flow rate, the values were considerably higher than those of untreated samples, suggesting that self-assembled films adsorbed on the stainless steel oxidized surface were resistant in the tested flow rates of seawater.

When examining the influence of the corrosive media, it can be assumed that it is mainly deter-

Table 3 – *Impedance parameters obtained for SS in river water*

		Q_f / μS s^n cm^{-2}	n_f	R_f / kΩ cm^2	Q_{ox} / μS s^n cm^{-2}	n_{ox}	R_{ox} / kΩ cm^2
SS	0 L min^{-1}	13.80	0.78	98.89	6.21	0.63	2655
	0.8 L min^{-1}	14.40	0.78	94.34	6.51	0.64	1976
	1.6 L min^{-1}	14.67	0.78	87.94	6.66	0.62	2031
	2.4 L min^{-1}	14.77	0.78	80.47	6.66	0.62	1789
ODPA/SS	0 L min^{-1}	0.25	0.96	3737	0.15	0.50	50550
	0.8 L min^{-1}	0.26	0.96	2979	0.18	0.50	46750
	1.6 L min^{-1}	0.27	0.96	2426	0.20	0.50	42250
	2.4 L min^{-1}	0.27	0.96	2202	0.21	0.50	37130

Table 4 – *Impedance parameters obtained for SS in seawater*

		Q_f / μS s^n cm^{-2}	n_f	R_f / kΩ cm^2	Q_{ox} / μS s^n cm^{-2}	n_{ox}	R_{ox} / kΩ cm^2
SS	0 L min^{-1}	33.98	0.86	5.08	85.61	0.58	566.3
	0.8 L min^{-1}	38.78	0.86	5.07	88.53	0.58	542.2
	1.6 L min^{-1}	40.44	0.86	4.85	91.13	0.58	539.1
	2.4 L min^{-1}	40.21	0.86	4.68	97.10	0.58	493.0
ODPA/SS	0 L min^{-1}	0.19	0.98	191.1	0.33	0.50	43360
	0.8 L min^{-1}	0.20	0.98	294.3	0.33	0.50	35460
	1.6 L min^{-1}	0.20	0.98	361.8	0.35	0.50	31660
	2.4 L min^{-1}	0.21	0.98	367.3	0.37	0.50	29010

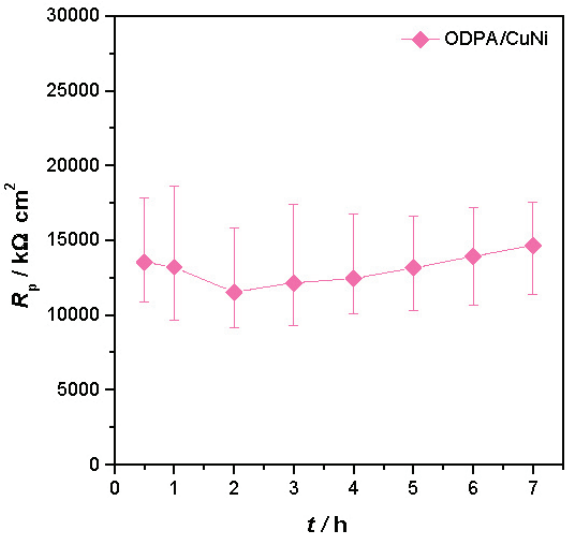

Fig. 11 – *Polarization resistance dependence on time of exposure to river water measured at a flow of 2.4 L* min^{-1}

mined by the chloride ion content of studied natural waters. It has significant influence on the corrosion behaviour of unprotected alloy, i.e., corrosion resistance of both alloys is much lower in seawater than in river water. On the other hand, seawater corrosion resistance of samples protected by SAM were two orders of magnitude greater than that of the blank sample, while in river water, the corrosion resistance of protected samples was just one order of magnitude greater than that of the blank sample. This implies that the ODPA layer efficiently protected underlying metallic substrates from the corrosive attack of chloride ions. Interestingly, the ODPA film on SS was much more resistant towards seawater flow than the film formed on CuNi, suggesting stronger attachment of ODPA on stainless steel than on the surface of CuNi alloy. It should also be taken into account that corrosion of both blank and protected CuNi in seawater was under partial mass transfer control as impedance spectra reveal Warburg diffusion impedance, characteristic for diffusion of chloride species from or into the solution. For other studied samples, low n_{dl}/n_{ox} values also indicated some influence of the mass transfer on corrosion rate; however, it appeared to be related to the diffusion through the film (ODPA or oxide), and was therefore less influenced by the electrolyte flow.

However, for CuNi alloy, an increase in seawater flow rate resulted in a more significant decrease in corrosion resistance of protected sample than in river water.

Influence of flow of medium in time

In order to determine the longevity of the protection at a constant flow rate, the samples were tested in time by polarization measurements in the narrow range of potentials, and the polarization resistance dependence on time of the exposure to river water is shown in Fig. 11.

Fig. 11, shows that, although there were some fluctuations in the R_p mean value during the 7-h test at the highest examined media flow rate, the ODPA film remained stable and lost none of its protective properties.

Conclusion

The results obtained in this work show that the protective films of ODPA could efficiently protect copper-nickel and stainless steel from corrosion in flowing natural waters (river and sea water). It was found that the flow rate had the highest impact on the corrosion resistance of the bare CuNi alloy in river water, which was attributed to the faster dissolution of corrosion products. For ODPA protected samples, the flow rate of the corrosive media had the highest influence on the stability of films on CuNi in seawater, while in all other studied cases, the protective properties of ODPA film changed insignificantly with the change in the flow rate.

ACKNOWLEDGMENTS

The research leading to these results received funding from the Croatian Science Foundation under grant agreement 9.01/253. The financial support of the Foundation of the Croatian Academy of Sciences and Arts, for projects "Corrosion protection of metals in natural waters" is gratefully acknowledged.

References

1. *Silverman, B. M., Wieghaus, K. A., Schwartz, J.,* Comparative properties of siloxane vs phosphonate monolayers on a key titanium alloy, Langmuir **21** (2005) 225. doi: https://doi.org/10.1021/la048227l
2. *Quiñones, R., Raman, A., Gawalt, E. S.,* Functionalization of nickel oxide using alkylphosphonic acid self-assembled monolayers, Thin Solid Films **516** (2008) 8774. doi: https://doi.org/10.1016/j.tsf.2008.06.055
3. *Dubey, M., Weidner, T., Gamble, L. J., Castner, D. G.,* Structure and order of phosphonic acid-based self-assembled monolayers on Si(100), Langmuir **26** (2010) 14747. doi: https://doi.org/10.1021/la1021438
4. *Hauffman, T., Hubin, A., Terryn, H.,* Study of the self-assembling of n-octylphosphonic acid layers on aluminum oxide from ethanolic solutions, Surf. Interface Anal. **45** (2013) 1435. doi: https://doi.org/10.1002/sia.5150
5. *Raman, A., Dubey, M., Gouzman, I., Gawalt, E. S.,* Formation of self-assembled monolayers of alkylphosphonic acid on the native oxide surface of SS316L, Langmuir **22** (2006) 6469. doi: https://doi.org/10.1021/la060636p
6. *Kristan Mioč, E.,* Longchain organic acids as corrosion inhibitors for steel and copper alloys in natural waters, doctoral thesis, Faculty of Chemical Engineering and Technology University of Zagreb, Zagreb, 2018, 79–181.
7. *Kristan Mioč, E., Hajdari Gretić, Z., Otmačić Ćurković, H.,* Modification of cupronickel alloy surface with octadecylphosphonic acid self–assembled films for improved corrosion resistance, Corros. Sci. **134** (2018) 189. doi: https://doi.org/10.1016/j.corsci.2018.02.021
8. *Vrsalović, L., Kliškić, M., Radošević, J., Gudić, S.,* The effect of electrolyte flow and temperature on corrosion and protection of Al-2.5 Mg alloy corrosion by (+)-catechin, J. Appl. Electrochem. **35** (2005)1059. doi: https://doi.org/10.1007/s10800-005-9015-9
9. *Martinez, S., Metikoš-Huković, M.,* The inhibition of copper-nickel alloy under controled hydrodynamic condition in sea water, J. Appl. Electrochem. **36** (2006) 1311. doi: https://doi.org/10.1007/s10800-005-9101-z
10. *Appa Rao, B. V., Chaitanya Kumar, K.,* Effect of hydrodynamic conditions on corrosion inhibition of Cu-Ni (90/19) alloy in seawater and sulphide containing seawater using 1,2,3-benzotriazole, J. Mater. Sci. Technol. **30** (2014) 65. doi: https://doi.org/10.1016/j.jmst.2013.08.019
11. *Ashassi-Sorkhabi, H., Asghari, E.,* Effect of solution hydrodynamics on corrosion inhibition performance of zinc sulfate in neutral solution, J. Electrochem. Soc. **159** (2012) C1. doi: https://doi.org/10.1149/2.006201jes
12. *Bommersbach, P., Alemany-Dumont, C., Millet, J. P., Normand, B.,* Formation and behaviour study of an environment-friendly corrosion inhibitor by electrochemical methods, Electrochim. Acta **51** (2006) 4011. doi: https://doi.org/10.1016/j.electacta.2005.06.001
13. *Stupnišek-Lisac, E., Galić, N., Gašparac, R.,* Corrosion inhibition of copper in hydrochloric acid under flow conditions, Corrosion **56** (2000) 1105. doi: https://doi.org/10.5006/1.3294395
14. *Babić, R., Metikoš-Huković, M., Lončar, M.,* Impedance and photoelectrochemical study of surface layers on Cu and Cu-10Ni in acetate solution containing benzotriazole, Electrochim. Acta **44** (1999) 2413. doi: https://doi.org/10.1016/S0013-4686(98)00367-3
15. *Starosvetsky, D., Sezin, N., Abelev, E., Cohen-Hyams, T., Ein-Eli, Y.,* Features of copper passivity in alkaline solutions at potentials below Cu_2O formation, J. Electrochem. Soc. **161** (2014) C77. doi: https://doi.org/10.1149/2.087401jes
16. *Kear, G., Barker, B. D., Walsh, F. C.,* Electrochemical corrosion of unalloyed copper in chloride media – a critical review, Corr. Sci. **46** (2004) 109. doi: https://doi.org/10.1016/S0010-938X(02)00257-3
17. *Crundwell, F. K.,* The anodic dissolution of copper in hydrochloric acid solutions, Electrocim. Acta **37** (1992) 2707. doi: https://doi.org/10.1016/0013-4686(92)85197-S
18. *Lee, H. P., Nobe, K.,* Kinetics and mechanisms of Cu electrodissolution in chloride media, J. Electrochem. Soc. **133** (1986) 2035. doi: https://doi.org/10.1149/1.2108335
19. *Deslouis, C., Tribollet, B., Mengoli, G., Musiani, M. M.,* Electrochemical behaviour of copper in neutral aerated chloride solution. I. Steady-state investigation, J. Appl. Electrochem. **18** (1988) 374. doi: https://doi.org/10.1007/BF01093751
20. *Deslouis, C., Tribollet, B., Mengoli, G., Musiani, M. M.,* Electrochemical behaviour of copper in neutral aerated chloride solution. II. Impedance investigation, J. Appl. Electrochem. **18** (1988) 384. doi: https://doi.org/10.1007/BF01093752
21. *Kear, G., Barker, B. D., Stokes, K., Walsh, F. C.,* Electrochemical behaviour of 90-10 Cu-Ni alloy in chloride-based electrolytes, J. Appl. Electrochem. **34** (2004) 659. doi: https://doi.org/10.1023/B:JACH.0000031164.32520.58
22. *Macdonald, J. R.,* Impedance spectroscopy, Emphasizing solid materials and systems, John Wiley & Sons, New York, 1987.
23. *Liu, C., Bi, Q., Leyland, A., Matthews, A.,* An electrochemical impedance spectroscopy study of the corrosion behaviour of PVD coated steels in 0.5 N NaCl aqueous solution: Part II.: EIS interpretation of corrosion behaviour, Corros. Sci. **45** (2003) 1257. doi: https://doi.org/10.1016/S0010-938X(02)00214-7
24. *Mansfeld, F., Liu, G., Xiao, H., Tsai, H., Little, B.,* The corrosion behavior of copper alloys, stainless steels and titanium in seawater, Corros. Sci. **36** (1994) 2063. doi: https://doi.org/10.1016/0010-938X(94)90008-6